colloids and interfaces

MDPI

Article

Encapsulation of Canola Oil by Sonication for the Development of Protein and Starch Systems: Physical Characteristics and Rheological Properties

Reynaldo J. Silva-Paz [1,*], Celenia E. Ñope-Quito [1], Thalia A. Rivera-Ashqui [2], Nicodemo C. Jamanca-Gonzales [1], Amparo Eccoña-Sota [3], Natalia Riquelme [4] and Carla Arancibia [4]

1 Departamento de Ingeniería, Escuela de Ingeniería en Industrias Alimentarias, Universidad Nacional de Barranca, Av. Toribio de Luzuriaga N° 376 Mz J-Urbanización La Florida, Barranca 15169, Peru; cnopeq162@unab.edu.pe (C.E.Ñ.-Q.); njamanca@unab.edu.pe (N.C.J.-G.)
2 CONICET—Consejo Nacional de Investigaciones Científicas y Técnicas, Godoy Cruz 2290, Buenos Aires C1425FQB, Argentina; thalia.rivera@conicet.gov.ar
3 Facultad de Medicina Veterinaria y Zootecnia, Universidad Nacional Micaela Bastidas de Apurímac, Av. Inca Garcilaso de la Vega s/n, Tamburco, Abancay, Apurímac 03001, Peru; aecconha@unamba.edu.pe
4 Department of Food Science and Technology, Universidad de Santiago de Chile, Obispo Umaña 050, Estación Central 9170201, Chile; natalia.riquelme.h@usach.cl (N.R.); carla.arancibia@usach.cl (C.A.)
* Correspondence: rsilva@unab.edu.pe; Tel.: +51-957805238

Abstract: Canola oil, extracted from *Brassica napus*, is appreciated for its nutritional profile, but its use in the food industry is limited by its susceptibility to oxidation. This study aimed to evaluate the nanoemulsion of canola oil by sonication to develop stable nanoemulsified gels from protein and starch systems. Two stages were performed. In the first stage, oil-in-water (O/W) nanoemulsions were prepared using soy lecithin and Tween 80 as emulsifiers, analyzing their physical stability by particle size and polydispersity index. The results show that the sonication conditions and emulsifier concentration significantly affected the creaming index and particle size. In the second stage, gels were developed from these nanoemulsions, evaluating their colorimetric and rheological properties. It was observed that the gels presented a viscoelastic behavior suitable for food applications, with a higher luminosity in protein systems. In conclusion, nanoemulsion by sonication improves the stability of canola oil, suggesting its potential use in various food applications. Additional emulsifier combinations and optimization of processing conditions are recommended to further improve the stability and functionality of the encapsulated oil.

Keywords: encapsulation; color; canola; optimization; rheology

check for updates

Academic Editors: Eleni P. Kalogianni and Julia Maldonado-Valderrama

Received: 8 November 2024
Revised: 12 December 2024
Accepted: 17 December 2024
Published: 22 January 2025

Citation: Silva-Paz, R.J.; Ñope-Quito, C.E.; Rivera-Ashqui, T.A.; Jamanca-Gonzales, N.C.; Eccoña-Sota, A.; Riquelme, N.; Arancibia, C. Encapsulation of Canola Oil by Sonication for the Development of Protein and Starch Systems: Physical Characteristics and Rheological Properties. *Colloids Interfaces* **2025**, *9*, 10. https://doi.org/10.3390/colloids9010010

Copyright: © 2025 by the authors. Licensee MDPI, Basel, Switzerland. This article is an open access article distributed under the terms and conditions of the Creative Commons Attribution (CC BY) license (https://creativecommons.org/licenses/by/4.0/).

1. Introduction

Canola oil, extracted from the Brassica napus plant, is valued for its exceptional nutritional profile, highlighting its monounsaturated fatty acid, omega-3, and antioxidant content. However, its application in the food industry faces challenges due to its susceptibility to oxidation and degradation during processing and storage [1]. To address this issue, encapsulation has emerged as an effective technique to protect and stabilize canola oil, thus preserving its nutritional and functional properties. This method allows for the formation of microcapsules containing small droplets of canola oil dispersed in a liquid or solid matrix, with potential applications in the food, pharmaceutical, and cosmetic industries. These microcapsules improve the stability, solubility, and bioavailability of canola oil in addition to protecting it from oxidation and other environmental factors. Canola oil has

been shown to be effective in reducing low-density lipoprotein cholesterol (LDL-C) and apolipoprotein B levels in overweight and obese individuals, which is useful in preventing and reducing the risk of atherosclerosis [2]. Furthermore, its consumption has beneficial effects on LDL-C, total cholesterol, and the LDL-C–HDL-C ratio compared with olive oil, suggesting cardioprotective impacts [3].

Nanoemulsions have gained popularity in the food industry because they are manufactured from generally recognized as safe (GRAS) ingredients, offering advantages such as improved water dispersibility of the encapsulated oils, excellent physical and chemical stability, and high bioavailability of the lipid components. However, these unstable colloidal dispersions formed by two immiscible phases require the use of emulsifiers that facilitate emulsification, promote physical stability, and can influence oxidative stability, especially when there is the presence of pro-oxidant compounds such as transition metals that can interact with lipids in the core of the emulsion droplets [4,5]. Tween 80, a nonionic synthetic emulsifier with a high hydrophile–lipophile balance (HLB) value of 15.0, is widely used in the preparation of nano- and macro emulsions due to its excellent emulsifying properties, although its consumption is limited to an acceptable daily intake (ADI) of 25 mg/kg (172,840, U.S. FDA) [6–8]. On the other hand, soy lecithin, composed of a mixture of phospholipids, triglycerides, glycolipids, and sterols, is the most widely used natural emulsifier in the food industry. It is water soluble and forms a colloidal suspension that favors the stability of oil–water emulsions due to its hydrophilic and hydrophobic groups [9,10]. Both synthetic and natural emulsifiers play a crucial role in the stabilization of oil–water emulsions by adsorbing at the interface and reducing the interfacial tension, protecting the droplets against aggregation and allowing for the formation of stable and bioavailable systems.

Encapsulation is a process by which particles or droplets of bioactive compounds are surrounded by polymeric compounds, such as proteins and/or polysaccharides, to form small capsules containing the active compound of interest. This method is used to isolate, protect, release in a controlled manner, or mask the taste and odor of compounds such as oils [11,12]. Among the most commonly encapsulated ingredients are flavorings, lipids, enzymes, microorganisms, leavening agents, antioxidants, preservatives, colorants, minerals, essential oils, and vitamins. However, these compounds can be sensitive to degradation by light, temperature, or pH [13].

Sonication encapsulation is a process that uses ultrasonic energy to create microcapsules containing active components. Sonication applies high-frequency ultrasonic waves to a liquid mixture, generating cavitation bubbles that collapse rapidly. This phenomenon produces intense shear and turbulence forces useful for emulsifying and encapsulating oils in the form of microdroplets. Sonication is widely used in industry due to its high energy and efficiency [14]. This method offers several advantages, such as a fast and efficient process, the ability to encapsulate heat-sensitive compounds, and the production of microcapsules with a uniform particle size (between 6 and 15 μm) [15]. However, optimizing sonication conditions, such as intensity, power, frequency, and exposure time, is crucial to ensure the optimal manufacturing of high-quality microcapsules [16]. The development of matrices is essential in encapsulation, and protein substances can be used due to their excellent emulsification capacity, biocompatibility, and biological activity [17]. Polysaccharides can also be used, which allow for encapsulation using natural products, such as chitosan, carrageenan, whey proteins, lupine protein isolate [11], alginate [18], gums, pectins, and gelatins, or synthetic products, such as polyvinyl alcohol, polyethylene glycol, and polylactic-co-glycolic acid [13]. The interactions between proteins and polysaccharides improve the stability and sensitivity of the microcapsules [17]. Recent research has explored the encapsulation of active ingredients, such as hyssop extract (*Hyssopus officinalis* L.), obtained by extraction

prior to ultrasound-assisted cold plasma treatment within a double emulsion stabilized with soy protein isolate (SPI) alone and combined with chia seed gum (CSG). In these studies, it was shown that canola oil containing encapsulated extract presented lower oxidative alterations than the non-encapsulated form [19]. In addition, tests have been performed on the antioxidant activity of aqueous extracts of *Bifurcaria bifurcata* (BBE) at different doses, compared to butylated hydroxytoluene (BHT) in canola oil, indicating that BBE may be a potential natural additive to improve the oxidative stability of canola oil [20]. In this context, the objective of this study was to evaluate the encapsulation of canola oil (*Brassica napus*) by sonication for the development of protein and starch systems in order to create stable nanoemulsified gels and determine the physical, colorimetric, and rheological stability of the encapsulated oil.

2. Materials and Methods

2.1. Materials

Oil-in-water (O/W) nanoemulsions were prepared using purified water from a reverse osmosis system (Vigaflow S.A., Santiago-Chile), canola oil (Belmont, Watt's SA, San Bernardo, Santiago, Chile), and two types of emulsifiers: soy lecithin (a natural emulsifier) (Metarin P-Cargill, Blumos SA, Santiago, Chile) and Tween 80 (a synthetic emulsifier) obtained from Sigma-Aldrich S.A. (St. Louis, CA, USA). In addition, protein isolate—WPI (Nutralys F85M, Lestron, France) and starch (Enterex Food, Santiago, Chile) were used for the preparation of the gels.

2.2. Stage 1

2.2.1. Preparation of Nanoemulsions

Oil-in-water (O/W) nanoemulsions were prepared using 5% canola oil and the emulsifiers soy lecithin (3% *w*/*w*) and Tween 80 at different concentrations (Table 1). The aqueous phase was prepared by dispersing Tween 80 in purified water using a magnetic stirrer (model Arex, Velp Scientifica, Usmate Velate, Italy) at 350 rpm for 10 min. Then, soy lecithin (3% *w*/*w*) was added to the aqueous phase and stirred for 40 min at 450 rpm until completely dispersed. Subsequently, canola oil was slowly added to the aqueous phase, while the mixture was homogenized at 12 000 rpm using a high-speed homogenizer (model IKA T25, Ultra Turrax, Germany) for 10 min. After adding all of the oil phase, the preemulsion was homogenized using an ultrasonic homogenizer (model VCX500, Sonics, Newtown, CT, USA) with a 13 mm diameter stainless steel ultrasound probe under conditions of 20 kHz, 90% amplitude, and between 5 and 20 min with work and rest intervals of 15 and 10 s, respectively. Finally, before measurements, the nanoemulsions were stored at 5 ± 1 °C for 24 h, with no destabilization phenomena observed under these conditions. The preparation procedure of the nanoemulsions was based on previous experiences in comparable rheological properties with similar products [4,21].

Table 1. Treatment formulation.

Treatment	Independent Variable			Dependent Variable
	Time (min)	Lecithin (g)	Tween 80 (g)	
1	12.5	2.45	0.3	Creaming index Particle size Polydispersion index
2	5.0	2.45	0.1	
3	12.5	0.40	0.5	
4	20.0	4.50	0.3	
5	20.0	2.45	0.5	
6	5.0	0.40	0.3	

Table 1. *Cont.*

Treatment	Independent Variable			Dependent Variable
	Time (min)	Lecithin (g)	Tween 80 (g)	
7	5.0	4.50	0.3	Creaming index Particle size Polydispersion index
8	20	0.40	0.3	
9	12.5	0.40	0.1	
10	12.5	2.45	0.3	
11	20.0	2.45	0.1	
12	12.5	2.45	0.3	
13	12.5	4.50	0.1	
14	5.0	2.45	0.5	
15	12.5	4.50	0.5	

2.2.2. Physical Properties for Determining Canola Oil Encapsulation

Particle Size Characterization and Polydispersity Index

The particle size and polydispersity index of different nanoemulsions were determined by dynamic light scattering (DLS) using a Zetasizer (NanoS90, Malvern Instruments, Malvern, UK). To perform the measurements, each nanoemulsion was diluted (50 µL of the nanoemulsion in 1 mL of milli-Q water) until a clear solution was obtained in order to reach a detectable concentration and avoid interference with the measurement. The particle size of the samples was described by the average particle size (PS), and the size distribution was described by the polydispersity index (PdI) [21]. The reported values are an average of 10 determinations and each sample was measured in triplicate (n = 3).

Physical Stability of Nanoemulsions

The instability of nanoemulsions during storage was characterized by the level of creaming, which is measured by the creaming index (H), where a high value of the creaming index is representative of a high degree of instability of the nanoemulsion. The creaming index was calculated according to Equation (1) as described by Petrovic et al. [22]:

$$Cream\ index\ (\%) = \frac{HS}{HE} \times 100\% \quad (1)$$

where HE is the total height of the nanoemulsion (mm) and HS is the height of the cream layer (mm), which was measured visually as a function of time. All measurements were performed in triplicate for each emulsion (n = 3).

2.2.3. Experimental Statistical Design

To evaluate the influence of sonication time, lecithin, and Tween 80, a Box–Behnken-type surface response design was used (Table 1). A total of 15 treatments were obtained (12 factorial points + 3 central points). From this design, a multiple response analysis was performed to find the optimal parameters for the physical stability of the nanoemulsion, which was applied in Stage 2.

2.3. Stage 2

2.3.1. Preparation of Nanoemulsion-Encapsulated Gels

For the preparation of gels with the nanoemulsion, the first step involved the formulation of the base nanoemulsion, which was optimized in the initial stage. This nanoemulsion consisted of 4 g of lecithin, 0.5 g of Tween 80, 5 g of canola oil, and 90.5 g of water sonicated for 10 min. Subsequently, different systems were prepared. The protein system, utilizing whey protein, was formulated at concentrations of 7.5, 10.0, 12.5, and 15.0%. In the case of the protein–starch mixture system, the protein concentration was kept constant at 3%,

while the starch percentages varied over 1, 2, 3, and 4%. All components were mixed with 5% of the base nanoemulsion, and the remainder of the formulation was adjusted with water according to each treatment. Dispersion was performed using a propeller stirrer (F20100151, Velp Scientifica, Usmate Velate, Italy) at 450 rpm in a thermoregulated bath (Heating bath B-100, Buchi, Flawil, Switzerland) at 90 ± 1 °C for 30 min. The dispersions obtained were then cooled to room temperature (25 ± 1 °C) and stored at 4 ± 1 °C for 24 h until further characterization.

2.3.2. Colorimetric and Rheological Properties

Colorimetric Properties of Nanoemulsion-Based Gels

The optical properties of the nanoemulsion-encapsulated gels were determined using a colorimeter (ChromaMeter CR-410, Konica Minolta, Osaka, Japan), which was calibrated with a standard calibrated plate (L*: 93.46, a*: 0.42, b*: 4.08). A 20 g piece of each sample was placed in a Petri dish (60 mm internal diameter) to homogenize the surface and obtain the CIELab parameters L* (brightness), a* (redness–greenness), and b* (blueness–yellowness).

Flow Properties of Nanoemulsion-Based Gels

The flow behavior of all nanoemulsions encapsulated in a protein system or starch–protein mixture was characterized using a rotational rheometer (MCR 72, Anton Paar, Austria) equipped with a concentric cylinder's geometry (CC50, Anton Paar, Austria). Flow curves were determined by recording the shear stress (τ) vs. shear rate (γ) values of the samples from 1 to 100 s^{-1} and from 100 to 1 s^{-1} for 120 s. Measurements were performed at 25 ± 1 °C, controlled with a Peltier system [23]. The sample liquids were placed and allowed to stand for 10 min before measurement to recover their structure and reach the test temperature. In addition, the consistency (K) and flow (n) index were determined using the power law (Equation (2)) in order to compare the flow parameters of the samples.

$$\tau = K \cdot \gamma^n \quad (2)$$

Viscoelastic Properties of Nanoemulsion-Based Gels

Viscoelastic testing of the nanoemulsion-encapsulated gels was carried out at 25 ± 1 °C using a controlled stress rheometer (MCR 72, Anton-Paar, Austria) equipped with a plate geometry (PP 50, 50 mm diameter, 1 mm gap). After loading the sample into the rheometer, it was allowed to stand for 10 min to stabilize and reach the test temperature. Small-amplitude oscillation sweeps were performed to analyze the viscoelastic properties of the samples. First, the linear viscoelasticity zone (LVR) was determined, where strain sweeps between 0.01 and 100% were performed at 1 Hz. Then, a frequency sweep from 0.1 to 10 Hz was performed at 0.1% strain, which was selected as it lies within the LVR. Finally, oscillatory rheological parameters (G′ and G″) were calculated at 1.17 Hz in order to compare the viscoelastic properties of the different nanoemulsion-encapsulated gels. Measurements were performed in triplicate (n = 3).

2.3.3. Experimental Statistical Design

A completely randomized design (CRD) was used to determine the differences between protein and starch systems (Table 2). Eight treatments were designed with different protein percentages and the protein–starch combination for the development of encapsulated gels with the base nanoemulsion.

Table 2. Formulation of nanoemulsion-based gel treatments.

Treatment	Independent Variable	Response Variables
Essay: Protein System (WPI)		Colorimetric parameters Rheological parameters
T1	7.5% WPI	
T2	10% WPI	
T3	12.5% WPI	
T4	15% WPI	
Essay: Protein–starch mixture system (ALM)		
T5	1% Starch + 3% WPI	
T6	2% Starch + 3% WPI	
T7	3% Starch + 3% WPI	
T8	4% Starch + 3% WPI	

2.4. Statistical Analysis

For the first stage, a three-factor ANOVA (analysis of variance) was performed using the Box–Behnken design and multi-response analysis of the creaming index, polydispersity index, and particle size. In the second stage, the colorimetric parameters and rheological properties were compared by applying the CRD through a one-way analysis and the Tukey test with a significance level of 95% using the R software. The experiments were performed in duplicate and each replicate was measured at least twice (minimum of four measurements). The results are reported as the average of all measurements and their corresponding standard deviation.

3. Results and Discussion

3.1. Stage 1—Physicochemical Characteristics of the Encapsulated Products

Table 3 presents the results obtained using the Box–Behnken design for the creaming index, particle size, and polydispersity index. Significant differences were found in the creaming index and particle size ($p > 0.05$), although it was not significant for the polydispersity index ($p > 0.05$). This design was used in several encapsulation studies [24–27]. These results are close to those obtained in peppermint oil emulsions stabilized with zein–lecithin complex nanoparticles with a particle size of 375 nm and a polydispersity index of 0.45 [28]. This difference is probably due to the type of encapsulation and the matrices used in the studies. Likewise, stable emulsions with canola protein isolates (*Brassica napus* L. var. *napus*), black caraway oil cake (*Nigella sativa*), and wheat bran (*Triticum aestivum*) produced lower and more consistent particle diameters [29]. Furthermore, nanoencapsulation of phenolic extract derived from the *Pimpinella affinis* plant, with *Salvia macrosiphon* gum and chitosan as coating agents, generated particle sizes between 75.8 and 144.2 nm and a variable polydispersity of 0.25 to 0.44 [30].

Table 4 shows the analysis of variance and the estimated regression coefficients corresponding to the physical stability parameters of the emulsions. For the creaming index, the model was significant ($p < 0.05$) for time (the quadratic term), lecithin concentration (the linear term), Tween 80 concentration (the linear and quadratic terms), and the time × Tween 80 interaction. The square term of time and Tween 80 concentration and the linear term of lecithin concentration significantly decreased ($p < 0.05$) the creaming index values, while the linear term of Tween 80 concentration and the time × Tween 80 interaction significantly increased it ($p < 0.05$). For the particle size parameter, the model was significant ($p < 0.05$). The lecithin concentration (linear and quadratic terms) and the Tween 80 concentration (linear term) significantly decreased ($p < 0.05$) this parameter. Regarding the polydispersity index, no significant effect ($p > 0.05$) of the factors and interactions

was observed. Abbasi et al. [30] indicated that the differences between the emulsifying properties (surface activity, plasticity properties) of the coating materials can influence the results on the particle size of the emulsions.

Table 3. Physicochemical characteristics of the encapsulated product.

Treatments	Creaming Index (%)	Particle Size (nm)	Polydispersity Index
1	1.0	196.400	0.21525
2	4.5	258.325	0.26050
3	2.0	266.475	0.21825
4	1.0	161.400	0.21275
5	7.5	137.900	0.15775
6	5.5	280.800	0.21500
7	1.0	177.425	0.18350
8	5.5	273.900	0.21000
9	3.5	267.575	0.20900
10	1.5	174.275	0.15025
11	2.0	209.050	0.17800
12	1.0	172.325	0.16100
13	1.0	187.675	0.20200
14	4.5	143.575	0.15800
15	1.0	134.350	0.19025

Table 4. Regression coefficients and analysis of variance for the regression models corresponding to the physical stability parameters of the emulsions.

Factor	Creaming Index		Particle Size (nm)		Polydispersity Index	
	Coefficient	*p*-Value	Coefficient	*p*-Value	Coefficient	*p*-Value
Time	0.125	1.000	−19.469	0.176	−0.015	0.613
Time × Time	−2.416	0.004	−7.788	0.379	−0.007	0.745
Lecithin	−3.125	0.004	−106.975	0.008	−0.016	0.584
Lecithin × Lecithin	0.333	0.156	−34.594	0.038	−0.023	0.331
Tween 80	1.000	0.039	−60.081	0.024	−0.031	0.332
Tween 80 × Tween 80	−1.041	0.0201	1.575	0.842	−0.006	0.761
Time × Lecithin	0.000	1.000	−4.563	0.765	0.017	0.672
Time × Tween 80	2.750	0.011	21.800	0.245	0.041	0.359
Lecithin × Tween 80	0.750	0.121	−26.112	0.190	−0.011	0.792
R^2	0.845		0.932		0.556	
Lack of fit	0.0246		0.1956		0.567496	

Figure 1 shows the contour and response surface plots of the factors that influence the creaming index and droplet size. Figure 1a shows that the creaming index is influenced by intermediate sonication times working with high lecithin concentrations. This is corroborated by the significant effect of the time x lecithin interaction (Table 4). Similar behavior was observed in the creaming index with the sonication time and the Tween 80 concentration (Figure 1b), where intermediate times and low and intermediate concentrations of Tween 80 produce lower creaming parameters. Figure 1c presents the contour plot of soy lecithin and Tween 80, where higher concentrations of soy lecithin and low and intermediate values of Tween 80 reduce this parameter. Likewise, the R^2 value suggests that the model explains well the variation in the creaming index. These results can be contrasted with studies that evaluate the stability of emulsions and their relationship with stabilizing agents such as lecithin and surfactants (Tween 80) that affect stability by reducing the creaming index by decreasing the aggregation of droplet-sized particles, since this depends

mainly on the type of thickener. Starch-based nanoemulsions showed lower particle size, polydispersity, and Z-potential values, close to zero [4].

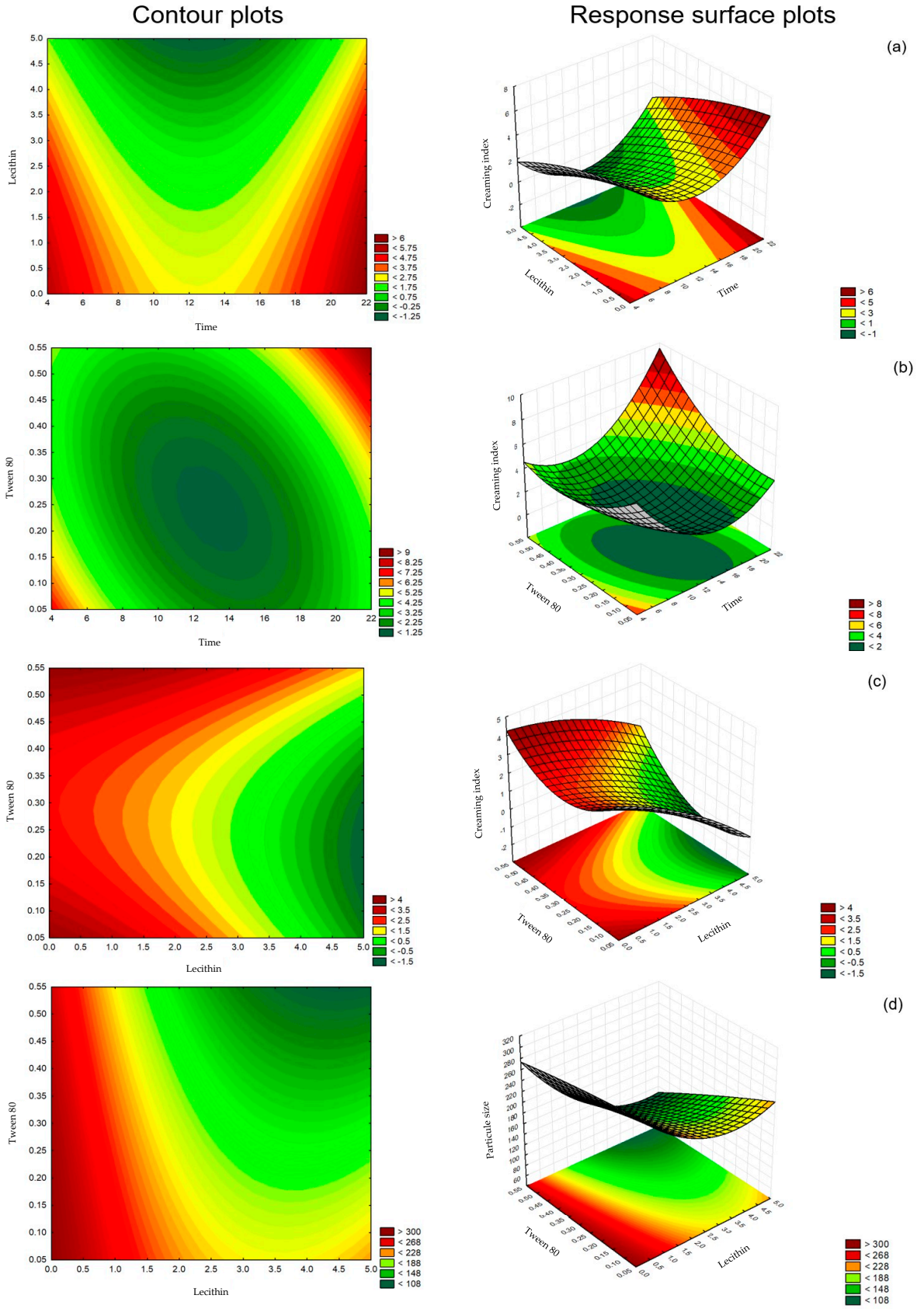

Figure 1. Contour plots and response surface for the creaming index. (**a**) Time vs. Lecithin, (**b**) Time vs. Tween 80, (**c**) Lecithin vs. Tween 80 and particle size, and (**d**) Lecithin vs. Tween 80.

Regarding particle size, Figure 1d presents the contour plot of soy lecithin and Tween 80, where higher soy lecithin concentrations and high Tween 80 values reduce this parameter. Furthermore, the negative coefficient of lecithin suggests that its addition significantly reduces the droplet size, which is consistent with its effect as an emulsifier. On the other hand, the R^2 shows that the model adequately describes the particle size (Table 4). These findings agree with studies on emulsions in which both lecithin and Tween 80 were used to stabilize and reduce the particle size. In works carried out with Tween 80 at a surfactant-to-oil ratio ≥ 1 at high stirring speeds (800 rpm), nanoemulsions with small particle diameters ($d < 200$ nm) were generated, being systems relatively stable to particle growth at room temperature (<10% of diameter after 1 month of storage) but unstable to heating ($T > 80$ °C) [7]. Also, extensive aggregation between oil particles gives rise to unstable emulsions due to the interactions produced [31].

Finally, as indicated, the polydispersity index is not significantly affected by any of the main factors or their interactions, since all *p* values are higher than 0.05. Furthermore, the lower R^2 also suggests that the model does not explain the variability in the polydispersity index as well. This could be interpreted as the formulations used providing sufficient stability, minimizing the differences in polydispersity.

In Figure 2, the graph generated by the desirability function is presented, which is one of the most used methods for optimizing the effect of multiple factors on a response variable. This method was developed by Harrington (1965) and modified by Derringer and Suich (1980), being applied in various studies on the optimization of encapsulation processes [32,33]. The desirability function was used to optimize the experimental design factors (lecithin, Tween 80 concentration, and sonication time) in order to obtain the desired values of the evaluated parameters. Figure 2 shows the graph of the analysis with the desirability function used to obtain the minimum value of the response variables for the development of the nanoemulsion. The conditions of the independent variables were 4.0 g of lecithin, 0.5 of Tween 80, and 10 min of sonication time, where the following predicted values were obtained for the response variables: a creaming index of 1.165%, a particle size of 135.081 nm, and a sonication time of 10 min.

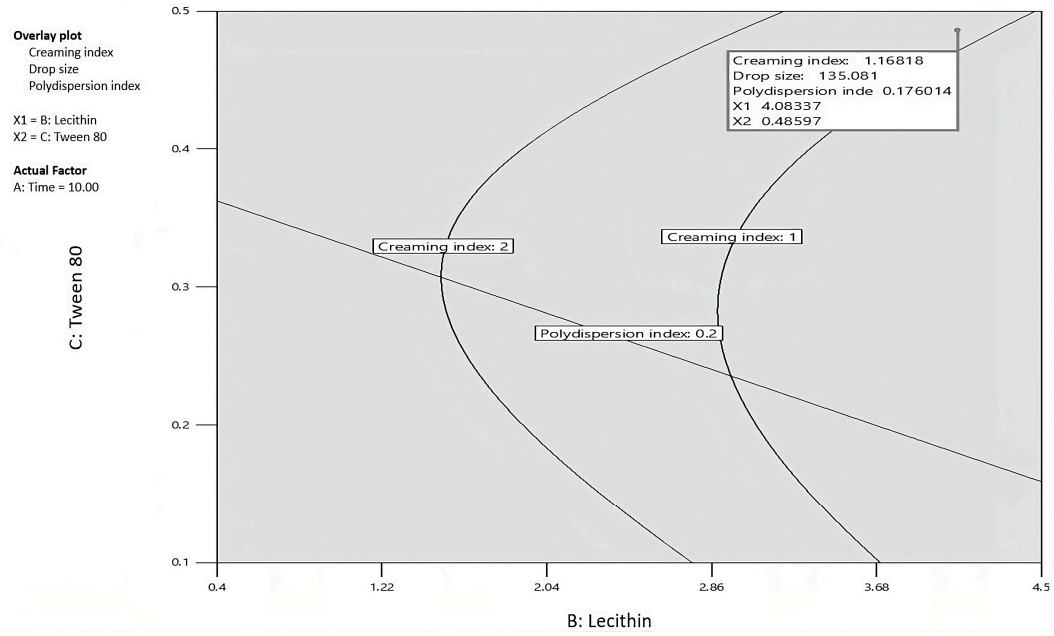

Figure 2. Multiple response analysis to find the optimal parameters for nanoemulsion development.

3.2. Stage 2—Colorimetric and Rheological Characteristics of the Gels with the Nanoemulsion

3.2.1. Colorimetric Parameters

The variance analysis of the emulsion's chromatic parameters is presented in Figure 3. We observed significant differences ($p < 0.05$) for the different treatments evaluated, mainly the concentrations of WPI alone and mixtures of starch with WPI. Considering the CIELab coordinates, the color of a gel with the nanoemulsion is generated when a beam of light hits the oil droplets and disperses the light. This depends largely on the oil concentration [34]. However, it is not the only factor that influences its appearance. The other components of the emulsion are also influential.

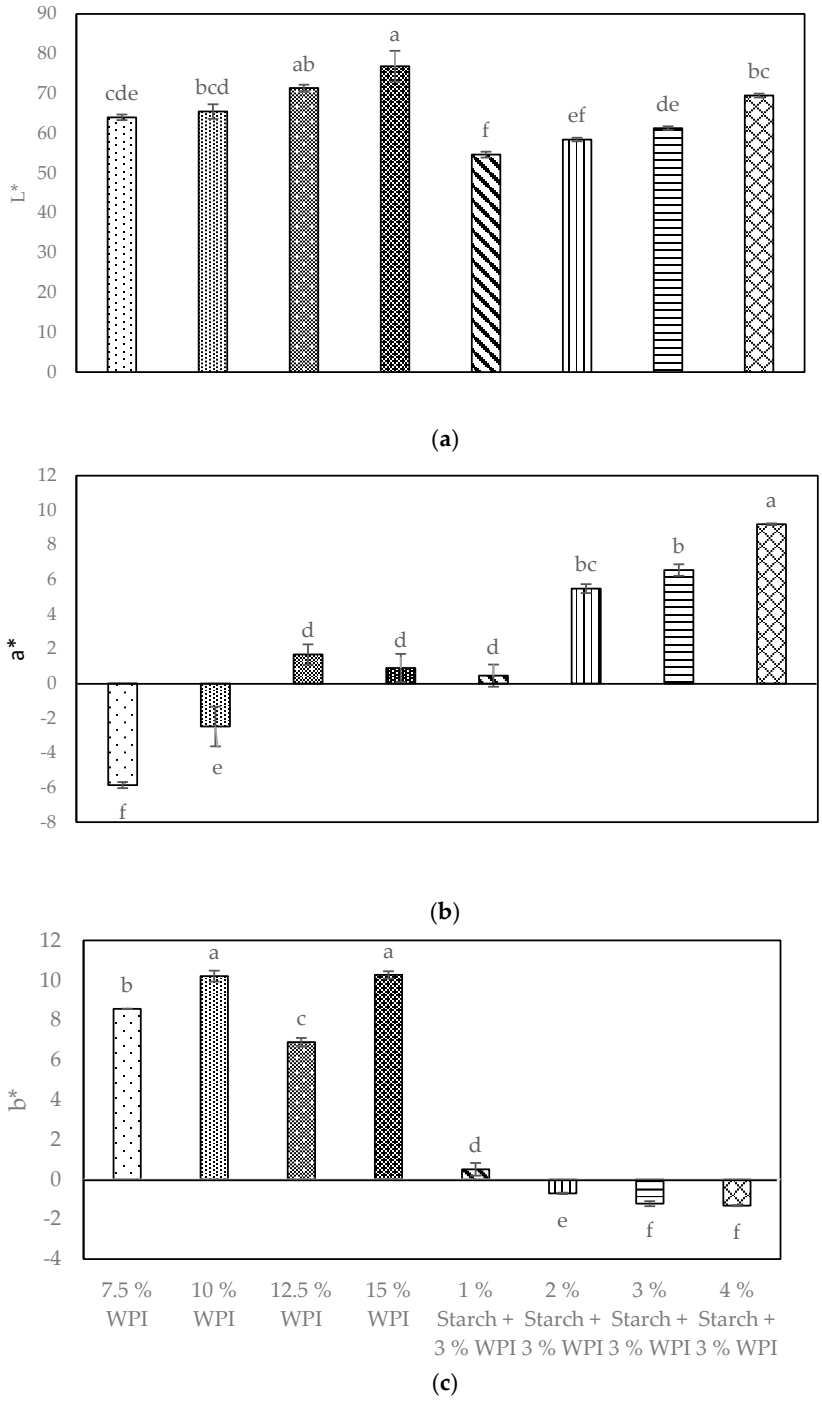

Figure 3. Colorimetric parameters of nanoemulsion-encapsulated gels. (**a**) L*, (**b**) a*, (**c**) b* (Note: [a,b,c,d,e,f] Different letters indicate significant differences).

The luminosity (L*) of the gel with the nanoemulsion was significantly higher ($p < 0.05$) due to the effect of the 12.5 and 15.0% WPI. In turn, the lowest values for this parameter were obtained due to the effect of 1% starch + 3% WPI and due to the effect of 2% starch + 3% WPI. In similar studies, the L* was influenced by the size of the drop, giving higher luminosity values when the diameter of the drop increases, generating greater light dispersion. On the other hand, smaller particles scatter less light [35].

The emulsion parameter a* decreased significantly ($p < 0.05$) due to the effect of the 7.5% WPI, while the highest value was obtained with 4% starch + 3% WPI. Therefore, the qualitative color obtained for the nanoemulsions was yellow. The a* values shown in Figure 3 ranged from −6 to 10. Because this variable varied linearly with increasing concentrations of WPI and starch, the values tended to be more positive, representing a shift toward red [36].

The parameter b* decreased significantly ($p < 0.05$) due to the effect of 3 and 4% starch + 3% WPI, while 10 and 15% WPI increased this parameter significantly ($p < 0.05$). The b* value, due to the qualitatively yellow color of the nanoemulsions, shifted toward blue (minimum b* values), fluctuating from −10 to 2 when the starch concentrations were high and the WPI concentrations were low [36].

3.2.2. Rheological Parameters

The results obtained on the rheological properties are presented in Figure 4. Specific behaviors were identified in the viscosity and shear stress of the samples analyzed at different shear rates and different concentrations of protein system gels and starch mixtures with WPI.

Figure 4a shows the relationship between shear rate and shear stress for different concentrations of proteinaceous gels (WPI) and starch–WPI blends (ALM). For all concentrations, the shear stress increased with the shear rate, being similar to the reduction in rheological properties in soy protein isolate and corn starch gels [37]. This indicates that WPI and ALM experience an increase in the stress required to deform as the shear rate increases. The differences in shear stress show that the 15% WPI sample and the 4% ALM sample have the highest shear stress values throughout the shear rate range. This suggests that both systems, at these concentrations, require higher stress to be deformed; thus, the gel strength is almost opposite to the viscosity order [38]. The lower concentrations of WPI (7.5, 10, and 12.5) show lower shear stresses than 15% WPI, but with a similar trend of increasing with the shear rate. In the case of ALM, the concentrations of 1, 2, and 3% show lower shear stress values compared with 4% ALM, but they also increase steadily with shear rate. The higher concentrations of both substances (WPI and ALM) have higher shear stress values, indicating that the resistance to deformation increases with concentration. WPI appears to be more sensitive to concentration than ALM in terms of shear stress, as the WPI samples exhibited a more pronounced increase in shear stress at higher concentrations.

Figure 4b shows the relationship between shear rate and viscosity for different concentrations of WPI and ALM-based emulsions. The shear behavior shows that, for each concentration, the viscosity decreases as the shear rate increases. This suggests that both WPI and ALM exhibit shear thinning behavior, meaning that they become less viscous when subjected to higher shear rates. The 15% WPI solution had the highest initial viscosity, starting above 14 000 mPa s and showing a steep drop as the shear rate increased. The lower WPI concentrations (7.5, 10, and 12.5%) showed decreasing initial viscosities with a similar decreasing trend as the shear rate increased. The starch solutions (1, 2, and 3% ALM) had lower initial viscosities than the WPI solutions at corresponding concentrations. However, among the WPI starch samples, the 4% ALM one had the highest viscosity, similar to the 15% WPI gel, while the 1% ALM gel had the lowest viscosity. Therefore,

higher concentrations of both WPI and ALM generally result in higher initial viscosities. WPI appears to have a more concentration-dependent viscosity response than ALM. It is evident that both WPI and ALM exhibit shear-thinning behavior, with WPI showing significantly higher viscosities at elevated concentrations compared with ALM.

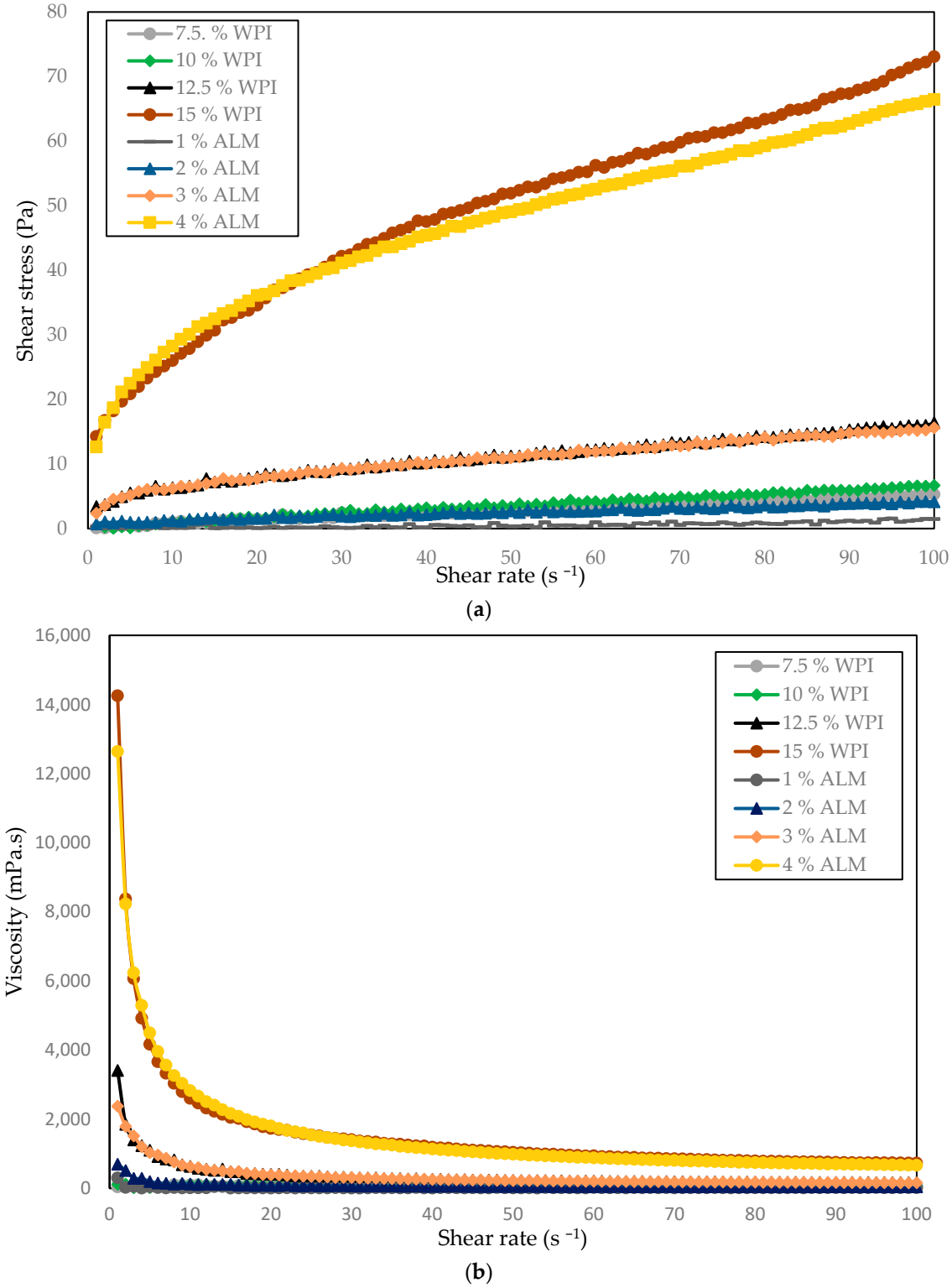

Figure 4. Flow curves of gels of protein systems and starch mixtures. (**a**) Shear stress vs. shear rate and (**b**) viscosity vs. shear rate.

Figure 5 shows the storage modulus G′ and the loss modulus G″ (in Pa) of different concentrations of WPI and ALM. The viscoelastic properties were determined within the linear viscoelasticity region (LVR) [38,39]. This allowed us to obtain more information on the structure of the gels at different concentrations of WPI and storage periods with WPI, managing to generate protein systems (WPI) and systems based on mixtures of starch and protein (ALM). The values of G′–G″ indicate the elasticity and viscosity of the material. The viscoelastic behavior indicated that G′ is significantly higher than G″. This indicates a predominance of elastic behavior in the network, which is desirable for structural applications. The viscoelasticity values were higher at higher concentrations (15% WPI and 4% ALM). Furthermore, the distance between G′ and G″ provides additional information about the network quality: a smaller distance suggests a more cohesive and stable structure [40]. The values of G′–G″ increased with frequency in all cases. As the WPI concentration increased (7.5 to 15%), the G′–G″ values also increased, indicating higher stiffness or elasticity at these higher concentrations. For ALM, a similar pattern was observed, where higher concentrations (e.g., 4% ALM) showed higher values in G′–G″, suggesting similar behavior in terms of elasticity and energy storage capacity. This behavior of both the elastic (G′) and viscous (G″) moduli of the gels increased linearly with increasing frequency, revealing a strong frequency dependence [41]. These results indicate that both systems (WPI and ALM) have the potential to form low-strength gels incorporating nanoemulsions, which require minimal force to bite and chew, easily disintegrating during processing in the mouth. Therefore, these gels are suitable for the development of food products with excellent textural properties.

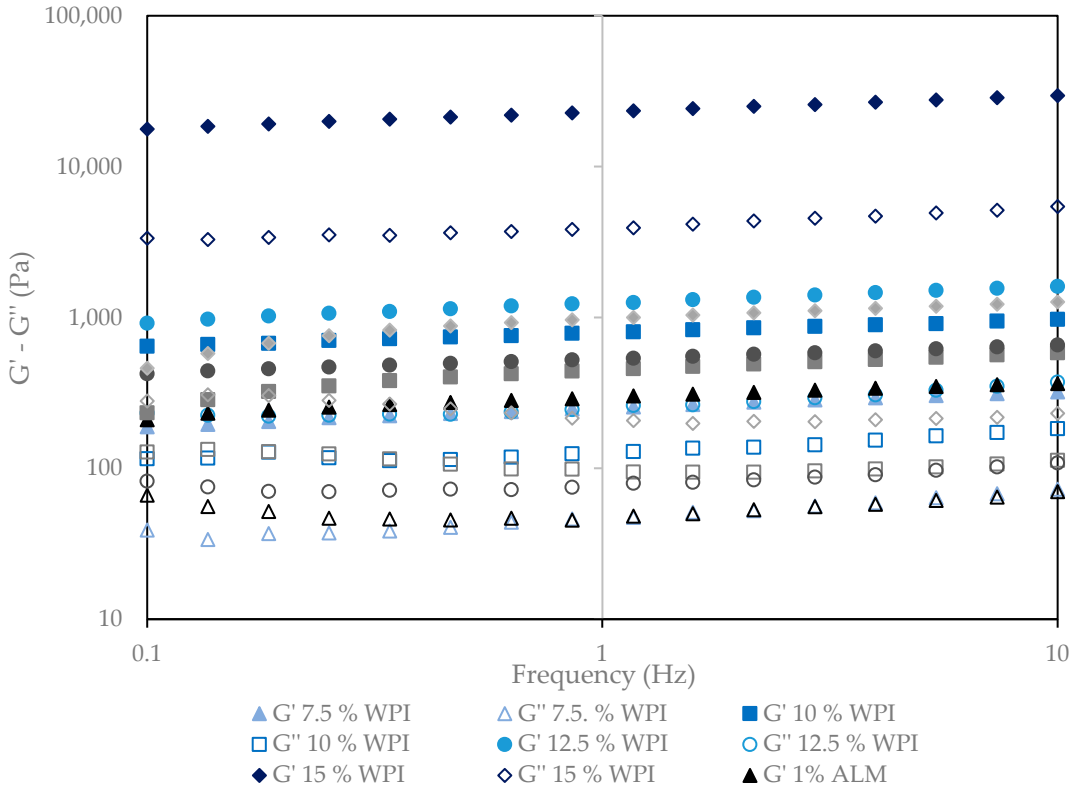

Figure 5. Frequency sweep from 0.1 to 10 Hz of gels of protein systems and starch mixtures.

In Table 5, the values of the rheological parameters of the protein (WPI) and starch–protein mixture (ALM) systems are shown. For the flow sweep data, the consistency index (K) and apparent viscosity were found to have significant differences ($p < 0.05$) between the treatments. The K values increased with the WPI concentration, from 0.086 at 7.5% to 11.069

at 15.0%. In the samples with ALM, it also increased with concentration, from 0.019 at 1.0% to 12.422 at 4.0%, suggesting that ALM has a greater capacity to form a more resistant structure at high concentrations. Regarding the flow index (n), it was found to be different between all treatments ($p < 0.05$). The n values for the WPI decreased with increasing concentration, going from 0.897 to 0.393, indicating that it becomes more pseudoplastic (stress-thinning flow). For ALM, it also decreased (from 0.826 at 1% to 0.355 at 4%), showing similar behavior. All treatments had a high R^2 (coefficient of determination) (close to 1), indicating a good fit of the data to the power law.

Table 5. Values of rheological parameters using the power law and constant frequency sweep.

Treatment	Flow Sweep—Power Law			Oscillatory Sweep—Frequency 1.17 Hz	
	K	n	R^2	G′	G″
T1: 7.5% WPI	0.086 ± 0.0002 ^{e}	0.897 ± 0.001 ^{a}	0.971 ± 0.0002	257.950 ± 3.320 ^{c}	47.793 ± 0.576 ^{g}
T2: 10% WPI	0.085 ± 0.0004 ^{e}	0.851 ± 0.0016 ^{b}	0.918 ± 0.0006	807.110 ± 4.790 ^{bc}	129.890 ± 0.997 ^{d}
T3: 12.5% WPI	2.781 ± 0.0016 ^{c}	0.364 ± 0.0015 ^{g}	0.981 ± 0.0006	1258.400 ± 2.400 ^{b}	262.080 ± 1.030 ^{b}
T4: 15% WPI	11.069 ± 0.0969 ^{b}	0.393 ± 0.0019 ^{e}	0.988 ± 0.0011	22,987.000 ± 685.00 ^{a}	3922.900 ± 9.05 ^{a}
T5: 1% Starch + 3% WPI	0.019 ± 0.0001 ^{e}	0.826 ± 0.0008 ^{c}	0.802 ± 0.0003	303.610 ± 1.970 ^{bc}	48.627 ± 0.528 ^{g}
T6: 2% Starch + 3% WPI	0.478 ± 0.0006 ^{d}	0.439 ± 0.0007 ^{d}	0.929 ± 0.0004	458.910 ± 1.820 ^{bc}	94.904 ± 0.560 ^{e}
T7: 3% Starch + 3% WPI	2.639 ± 0.0016 ^{c}	0.374 ± 0.0006 ^{f}	0.987 ± 0.0003	528.060 ± 2.740 ^{bc}	78.503 ± 0.703 ^{f}
T8: 4% Starch + 3% WPI	12.422 ± 0.0318 ^{a}	0.355 ± 0.0001 ^{h}	0.997 ± 0.0003	1000.900 ± 1.520 ^{bc}	208.110 ± 0.559 ^{c}

$^{a–h}$ Different letters indicate significant differences.

For the frequency sweep, G′ represents the storage modulus, which is the elasticity of the material or the ability to store energy. In the case of WPI, the G′ increased remarkably with concentration, from 257.95 at 7.5% to 22,987 at 15%, showing a significant increase in elasticity. For ALM, the G′ also increased with concentration, although the values were lower than those of the WPI at high concentrations. The maximum value in ALM was 1000.9 at 4%. In addition, G′ represents the loss modulus, which represents the viscosity of the material or its ability to dissipate energy. In the WPI, the G″ also increased with concentration, from 47.79 at 7.5% to 3922.9 at 15%. In the ALM, the G″ also increased with concentration, although with lower values than in the WPI, reaching a maximum of 208.11 at 4.0%. On the other hand, the elastic modulus (G′) was generally higher in the WPI than in the ALM. This indicates that WPI exhibits greater elasticity and stiffness compared with ALM, especially at high concentrations. This behavior suggests that WPI has a superior ability to recover its original shape after deformation, contributing to a more stable structure in applications where mechanical strength is required. Likewise, the viscosity (G″) indicated that the G″ values are also higher in WPI, suggesting that WPI has a higher energy dissipation capacity than ALM. WPI seems to form a stronger viscoelastic network compared with ALM, especially at higher concentrations. At all concentrations, the G′ values exceeded the G″ values, indicating elastic solid behavior with stable and well-structured networks [41]. Both the G′ values and G″ values increased with frequency, meaning that the gel network structure may be formed through non-covalent interactions [40].

4. Conclusions

Nanoemulsions present physicochemical characteristics that are significantly influenced by the concentration of lecithin and Tween 80, as well as by the sonication time, which translates into a reduced particle size and an optimized creaming index through a Box–Behnken experimental design. A higher concentration of lecithin and Tween 80 reduces the droplet size, which is consistent with its function as an effective and stable long-term emulsifier. The desirability function used to optimize the experimental conditions allowed us to identify formulations that maximize stability, highlighting the potential

of these nanoemulsions to improve the functional quality in food products. Gels with nanoemulsions made from whey protein isolate (WPI) and starch mixtures with WPI (ALM) present colorimetric and rheological characteristics that are significantly influenced by the concentration of lecithin and Tween 80, as well as by the sonication time. An increase in WPI concentration increases the lightness and affects the colorimetric parameters, resulting in emulsions with a more pronounced yellow color. Furthermore, the rheological properties indicate that both WPI and starch exhibit shear thinning behavior, being more pronounced at high concentrations, suggesting that these gels are suitable for food applications where a smooth texture and rapid disintegration are required.

Author Contributions: Conceptualization, methodology, and writing—original draft preparation, C.A. and R.J.S.-P.; data curation, C.A., N.R. and T.A.R.-A.; resources, C.E.Ñ.-Q. and N.C.J.-G.; statistical analysis, R.J.S.-P. and A.E.-S.; formal analysis, R.J.S.-P. and C.A.; writing—review and editing and visualization, R.J.S.-P., N.C.J.-G., T.A.R.-A. and C.A.; supervision, validation, project administration, and funding acquisition, R.J.S.-P. All authors have read and agreed to the published version of the manuscript.

Funding: This research was funded by Advanced Studies of the National Council for Science, Technology, and Technological Innovation (PROCIENCIA-CONCYTEC) through contract No. PE501082112-2023-PROCIENCIA for Applied Research Projects.

Institutional Review Board Statement: Not applicable.

Informed Consent Statement: Not applicable.

Data Availability Statement: The original contributions presented in the study are included in the article. Further inquiries can be directed to the corresponding authors.

Acknowledgments: This research was developed at the facilities of the National University of Barranca and the University of Santiago de Chile with funding from the National Program for Scientific Research.

Conflicts of Interest: The authors declare no conflicts of interest.

References

1. Enns, J.E.; Zahradka, P.; Guzman, R.P.; Baldwin, A.; Foot, B.; Taylor, C.G. Randomized controlled trial to evaluate the effect of canola oil on blood vessel function in peripheral arterial disease: Rationale and design of the Canola-PAD Study. *Open Access J. Clin. Trials* **2014**, *6*, 117–125.
2. Yang, J.-M.; Long, Y.; Ye, H.; Wu, Y.-L.; Zhu, Q.; Zhang, J.-H.; Huang, H.; Zhong, Y.-B.; Luo, Y.; Wang, M.-Y. Effects of rapeseed oil on body composition and glucolipid metabolism in people with obesity and overweight: A systematic review and meta-analysis. *Eur. J. Clin. Nutr.* **2024**, *78*, 6–18. [CrossRef]
3. Pourrajab, B.; Sharifi-Zahabi, E.; Soltani, S.; Shahinfar, H.; Shidfar, F. Comparison of canola oil and olive oil consumption on the serum lipid profile in adults: A systematic review and meta-analysis of randomized controlled trials. *Crit. Rev. Food Sci. Nutr.* **2023**, *63*, 12270–12284. [CrossRef]
4. Arancibia, C.; Miranda, M.; Matiacevich, S.; Troncoso, E. Physical properties and lipid bioavailability of nanoemulsion-based matrices with different thickening agents. *Food Hydrocoll.* **2017**, *73*, 243–254. [CrossRef]
5. Alipour, E.; Halverson, D.; McWhirter, S.; Walker, G.C. Phospholipid Bilayers: Stability and Encapsulation of Nanoparticles. *Annu. Rev. Phys. Chem.* **2017**, *68*, 261–283. [CrossRef] [PubMed]
6. McClements, D.J. Nanoemulsion-based oral delivery systems for lipophilic bioactive components: Nutraceuticals and pharmaceuticals. *Ther. Deliv.* **2013**, *4*, 841–857. [CrossRef] [PubMed]
7. Guttoff, M.; Saberi, A.H.; Mcclements, D.J. Formation of vitamin D nanoemulsion-based delivery systems by spontaneous emulsification: Factors affecting particle size and stability. *Food Chem.* **2015**, *171*, 117–122. [CrossRef] [PubMed]
8. Raikos, V. Encapsulation of vitamin E in edible orange oil-in-water emulsion beverages: Influence of heating temperature on physicochemical stability during chilled storage. *Food Hydrocoll.* **2017**, *72*, 155–162. [CrossRef]
9. Mezdour, S.; Desplanques, S.; Relkin, P. Effects of residual phospholipids on surface properties of a soft-refined sunflower oil: Application to stabilization of sauce-types' emulsions. *Food Hydrocoll.* **2011**, *25*, 613–619. [CrossRef]

10. Ozturk, B.; McClements, D. Progress in natural emulsifiers for utilization in food emulsions. *Curr. Opin. Food Sci.* **2016**, *7*, 1–6. [CrossRef]
11. Morales, E.; Burgos-Díaz, C.; Zúñiga, R.N.; Jorkowski, J.; Quilaqueo, M.; Rubilar, M. Influence of O/W emulsion interfacial ionic membranes on the encapsulation efficiency and storage stability of powder microencapsulated astaxanthin. *Food Bioprod. Process.* **2021**, *126*, 143–154. [CrossRef]
12. CGNA (Director). Microencapsulación: Una Tecnología que Potencia la Calidad y la Innovación de los Alimentos. Available online: https://www.youtube.com/watch?v=iYWeBJOWX10 (accessed on 10 August 2024).
13. Barbosa-Nuñez, J.A.; Espinosa-Andrews, H.; Cardona AA, V.; Haro-González, J.N. Polymer-based encapsulation in food products: A comprehensive review of applications and advancements. *J. Future Foods* **2025**, *5*, 36–49. [CrossRef]
14. Deng, R.-X.; Zheng, Y.-Y.; Liu, D.-J.; Liu, J.-Y.; Zhang, M.-N.; Xi, G.-Y.; Song, L.-L.; Liu, P. The effect of ultrasonic power on the physicochemical properties and antioxidant activities of frosted figs pectin. *Ultrason. Sonochem.* **2024**, *106*, 106883. [CrossRef]
15. Ho, J.; Wang, H.; Forde, G.M. Process considerations related to the microencapsulation of plasmid DNA via ultrasonic atomization. *Biotechnol. Bioeng.* **2008**, *101*, 172–181. [CrossRef]
16. Qu, W.; Feng, Y.; Xiong, T.; Qayum, A.; Ma, H. Preparation, structural and functional characterization of corn peptide-chelated calcium microcapsules using synchronous dual frequency ultrasound. *Ultrason. Sonochem.* **2024**, *102*, 106732. [CrossRef]
17. Ma, D.; Yang, B.; Zhao, J.; Yuan, D.; Li, Q. Advances in protein-based microcapsules and their applications: A review. *Int. J. Biol. Macromol.* **2024**, *263*, 129742. [CrossRef]
18. Piornos, J.A.; Burgos-Díaz, C.; Morales, E.; Rubilar, M.; Acevedo, F. Highly efficient encapsulation of linseed oil into alginate/lupin protein beads: Optimization of the emulsion formulation. *Food Hydrocoll.* **2017**, *63*, 139–148. [CrossRef]
19. Ahmadian, S.; Kenari, R.E.; Amiri, Z.R.; Sohbatzadeh, F.; Khodaparast MH, H. Fabrication of double nano-emulsions loaded with hyssop (*Hyssopus officinalis* L.) extract stabilized with soy protein isolate alone and combined with chia seed gum in controlling the oxidative stability of canola oil. *Food Chem.* **2024**, *430*, 137093. [CrossRef]
20. Agregán, R.; Lorenzo, J.M.; Munekata PE, S.; Dominguez, R.; Carballo, J.; Franco, D. Assessment of the antioxidant activity of Bifurcaria bifurcata aqueous extract on canola oil. Effect of extract concentration on the oxidation stability and volatile compound generation during oil storage. *Food Res. Int.* **2017**, *99*, 1095–1102. [CrossRef] [PubMed]
21. Arancibia, C.; Navarro-Lisboa, R.; Zúniga, R.N.; Matiacevich, S. Application of CMC as thickener on nanoemulsions based on olive oil: Physical properties and stability. *Int. J. Polym. Sci.* **2016**, *2016*, 6280581. [CrossRef]
22. Petrovic, L.B.; Sovilj, V.J.; Katona, J.M.; Milanovic, J.L. Influence of polymer-surfactant interactions on o/w emulsion properties and microcapsule formation. *J. Colloid Interface Sci.* **2010**, *342*, 333–339. [CrossRef] [PubMed]
23. Wang, Q.; Zhang, F.; Wang, S.; Chen, W.; Li, X.; Hao, J.; Alouk, I.; Wang, Y.; Xu, D.; Sun, B. The fabrication, microstructure, rheological properties and interactions of soft solid oleogels of hazelnut oil body. *Food Hydrocoll.* **2025**, *159*, 110711. [CrossRef]
24. Feczkó, T.; Tóth, J.; Dósa, G.; Gyenis, J. Optimization of protein encapsulation in PLGA nanoparticles. *Chem. Eng. Process. Process Intensif.* **2011**, *50*, 757–765. [CrossRef]
25. Bouriche, S.; Cózar-Bernal, M.J.; Rezgui, F.; Álvarez, A.M.R.; González-Rodríguez, M.L. Optimization of preparation method by W/O/W emulsion for entrapping metformin hydrochloride into poly (lactic acid) microparticles using Box-Behnken design. *J. Drug Deliv. Sci. Technol.* **2019**, *51*, 419–429. [CrossRef]
26. Essifi, K.; Lakrat, M.; Berraaouan, D.; Fauconnier, M.-L.; El Bachiri, A.; Tahani, A. Optimization of gallic acid encapsulation in calcium alginate microbeads using Box-Behnken Experimental Design. *Polym. Bull.* **2021**, *78*, 5789–5814. [CrossRef]
27. Sharaf, N.S.; Shetta, A.; Elhalawani, J.E.; Mamdouh, W. Application of Box-Behnken design for the formulation and optimization of coffee and PLGA nanoparticles and detection of enhanced antioxidant and anticancer activities. *Polymers* **2022**, *14*, 144. [CrossRef]
28. Xie, H.; Ni, F.; Gao, J.; Liu, C.; Shi, J.; Ren, G.; Tian, S.; Lei, Q.; Fang, W. Preparation of zein-lecithin-EGCG complex nanoparticles stabilized peppermint oil emulsions: Physicochemical properties, stability and intelligent sensory analysis. *Food Chem.* **2022**, *383*, 132453. [CrossRef] [PubMed]
29. Aktaş, H.; Custodio-Mendoza, J.; Moczkowska-Wyrwisz, M.; Szpicer, A.; Kurek, M.A. The role of canola, black caraway, and wheat bran protein isolates in anthocyanin microencapsulation via double emulsions. *Ind. Crops Prod.* **2024**, *222*, 119644. [CrossRef]
30. Abbasi, H.; Tavakoli, J.; Zare, F.; Salmanpour, M. Improving the efficacy of phenolic extract from *Pimpinella affinis* in edible oils through nanoencapsulation: Utilizing chitosan and *Salvia macrosiphon* gum as coating agents. *Food Sci. Nutr.* **2024**, *12*, 5463–5472. [CrossRef]
31. Paximada, P.; Koutinas, A.A.; Scholten, E.; Mandala, I.G. Effect of bacterial cellulose addition on physical properties of WPI emulsions. Comparison with common thickeners. *Food Hydrocoll.* **2016**, *54*, 245–254. [CrossRef]
32. Li, X.; Wang, L.; Wang, B. Optimization of encapsulation efficiency and average particle size of *Hohenbuehelia serotina* polysaccharides nanoemulsions using response surface methodology. *Food Chem.* **2017**, *229*, 479–486. [CrossRef] [PubMed]

33. Pashazadeh, H.; Zannou, O.; Ghellam, M.; Koca, I.; Galanakis, C.M.; Aldawoud, T.M. Optimization and encapsulation of phenolic compounds extracted from corn waste by freeze-drying, spray drying and microwave drying using maltodextrin. *Foods* **2021**, *10*, 1396. [CrossRef]
34. Salvia-Trujillo, L.; Rojas-Graü, M.A.; Soliva-Fortuny, R.; Martín-Belloso, O. Use of antimicrobial nanoemulsions as edible coatings: Impact on safety and quality attributes of fresh-cut Fuji apples. *Postharvest Biol. Technol.* **2015**, *105*, 8–16. [CrossRef]
35. McClements, D.J. Colloidal basis of emulsion color. *Curr. Opin. Colloid Interface Sci.* **2002**, *7*, 451–455. [CrossRef]
36. Ricaurte, L.; de Jesús Perea-Flores, M.; Martinez, A.; Quintanilla-Carvajal, M.X. Production of high-oleic palm oil nanoemulsions by high-shear homogenization (microfluidization). *Innov. Food Sci. Emerg. Technol.* **2016**, *35*, 75–85. [CrossRef]
37. Pi, X.; Zhu, L.; Xiang, M.; Zhao, S.; Cheng, Z.; Qiao, D.; Zhang, B. Insight of soy protein isolate to decrease the gel properties corn starch based binary system: Rheological and structural investigation. *Food Hydrocoll.* **2025**, *160*, 110750. [CrossRef]
38. Fu, J.; Cai, X.; Yang, Y.; Xie, H.; Duan, Q.; Liu, H.; Yu, L. Application of various polysaccharide gums to improve gelation and rheological properties of hydroxypropyl starch hydrocolloids. *Food Hydrocoll.* **2024**, *154*, 110043. [CrossRef]
39. Liang, X.; Ma, C.; Yan, X.; Zeng, H.; McClements, D.J.; Liu, X.; Liu, F. Structure, rheology and functionality of whey protein emulsion gels: Effects of double cross-linking with transglutaminase and calcium ions. *Food Hydrocoll.* **2020**, *102*, 105569. [CrossRef]
40. Farooq, S.; Ahmad, M.I.; Zhang, Y.; Chen, M.; Zhang, H. Preparation, characterization and digestive mechanism of plant-derived oil bodies-based oleogels structured by chitosan and vanillin. *Food Hydrocoll.* **2023**, *136*, 108247. [CrossRef]
41. Mert, B.; Vilgis, T.A. Hydrocolloid coated oleosomes for development of oleogels. *Food Hydrocoll.* **2021**, *119*, 106832. [CrossRef]

Disclaimer/Publisher's Note: The statements, opinions and data contained in all publications are solely those of the individual author(s) and contributor(s) and not of MDPI and/or the editor(s). MDPI and/or the editor(s) disclaim responsibility for any injury to people or property resulting from any ideas, methods, instructions or products referred to in the content.